Ambiente & Água - An Interdisciplinary Journal of Applied Science
ISSN 1980-993X – doi:10.4136/1980-993X
www.ambi-agua.net
E-mail: ambi.agua@gmail.com

Continuous process for the effective removal of gasoline from an aqueous emulsion using mexicalcite as an adsorbent in a packed bed column

ARTICLES doi:10.4136/ambi-agua.3088

Received: 30 May 2025; Accepted: 16 Dec. 2025

Julian Cruz-Olivares[1]; César Pérez-Alonso[2];
Eduardo Martín del Campo-López[2*]

[1]Departamentos de Ingeniería Química e Ingeniería Petroquímica. Facultad de Química. Universidad Autónoma del Estado de México, Paseo Colón esquina Paseo Tollocan, s/n, 50120, Toluca, Estado de México, México.
E-mail: jcruzo@uaemex.mx
[2]Departamento de Ingeniería Química. Facultad de Química. Universidad Autónoma del Estado de México, Paseo Colón esquina Paseo Tollocan, s/n, 50120, Toluca, Estado de México, México.
E-mail: cpereza@uaemex.mx
[*]Corresponding author. E-mail: emartindelcampol@uaemex.mx

Editor-in-Chief: Nelson Wellausen Dias

ABSTRACT

Thanks to its extraordinary properties as an adsorbent, the mineral called “mexicalcite” was used to remove gasoline from a water emulsion in a continuous process. A glass column with an internal diameter of 1.6 cm was used to analyze the effect of the packed bed height (Z), flow rate (Q) and the influent concentration (C_0) on the percentage of gasoline removal ($\%R$) and the adsorption capacity (q). The experimental results show that the effect of Z, Q, and C_0 is positive on the adsorption capacity, that is, an increase in the value of these three factors causes an increase in the amount of adsorbed gasoline. The only negative effect was found when the volumetric flow rate was modified; in this case, the percentage of gasoline removal decreased 8.7 and 15.4% when increased from 5 to 10 mL·min^{-1} and from 5 to 15 mL·min^{-1}, respectively. Experimentally, the highest removal percentage (97.1%) and maximum adsorption capacity (132.23 mg·g^{-1}) were obtained with a packed bed height of 4 cm, a volumetric flow rate of 5 mL·min^{-1} and an initial concentration of 1500 mg·L^{-1}. The continuous process was successfully modeled using the Thomas, Adams-Bohart, Wolborska, Dose-Response, and Yoon-Nelson models. The Thomas and Dose-Response models yielded a maximum adsorption capacity of 125.31 mg·g^{-1}. These results demonstrate that mexicalcite is a potential adsorbent for gasoline removal from water.

Keywords: adsorption capacity, gasoline removal, packed bed column, removal percentage, Thomas model.

Processo contínuo para a remoção eficaz de gasolina de uma emulsão aquosa utilizando mexicalcita como adsorvente em uma coluna de leito fixo

RESUMO

Graças às suas extraordinárias propriedades como adsorvente, o mineral chamado mexicalcita foi usado para remover gasolina de uma emulsão aquosa em um processo contínuo. Uma coluna de vidro com diâmetro interno de 1.6 cm foi utilizada para analisar o efeito da profundidade do leito (Z), vazão (Q) e concentração do afluente (C_0) na porcentagem de remoção de gasolina ($\%R$) e na capacidade de adsorção (q). Os resultados experimentais mostram que o efeito de Z, Q e C_0 é positivo na capacidade de adsorção, ou seja, um aumento no valor desses três fatores causa um aumento na quantidade de gasolina adsorvida. O único efeito negativo foi encontrado quando a vazão volumétrica foi modificada; neste caso, a porcentagem de remoção de gasolina diminuiu ligeiramente (8.7 e 15.4%) quando aumentada de 5 para 10 $\text{mL}\cdot\text{min}^{-1}$ e de 5 para 15 $\text{mL}\cdot\text{min}^{-1}$, respectivamente. Experimentalmente, a maior porcentagem de remoção (97.1%) e a capacidade máxima de adsorção (132.23 $\text{mg}\cdot\text{g}^{-1}$) foram obtidas com uma altura de leito fixo de 4 cm, uma vazão volumétrica de 5 $\text{mL}\cdot\text{min}^{-1}$ e uma concentração inicial de 1500 $\text{mg}\cdot\text{L}^{-1}$. O processo contínuo foi modelado com sucesso utilizando os modelos de Thomas, Adams-Bohart, Wolborska, Dose-Resposta e Yoon-Nelson. Os modelos de Thomas e Dose-Resposta produziram uma capacidade máxima de adsorção de 125.31 $\text{mg}\cdot\text{g}^{-1}$. Esses resultados posicionam a mexicalcita como um adsorvente competitivo para a remoção de gasolina da água.

Palavras-chave: capacidade de adsorção, coluna de leito fixo, modelo de Thomas, porcentagem de remoção, remoção de gasolina.

1. INTRODUCTION

Hydrocarbon-related water contamination is a continuous and worldwide environmental problem that results from a confluence of natural disasters, infrastructural failures, and operational mishaps. The severity of this problem is demonstrated by recurring incidents that endanger water security in various locations. For instance, recent high-impact events in Mexico have confirmed the vulnerability of water sources: in October 2025, a meteorological phenomenon caused a crude oil spill that affected the Pantepec River (Puebla and Veracruz) (Morales, 2025), and in July 2023, a light crude oil leak was recorded in a pipeline at the Ek Balam field in the Bay of Campeche (Arellano, 2023).

Gasoline presents a particularly serious harm to the environment. Due to its handling and extensive storage in refineries and distribution facilities, gasoline, the most commonly used vehicle fuel worldwide, is commonly involved in spills and leaks that pollute land and bodies of water, including groundwater, lakes, rivers, and oceans. Large facilities are not the only places where this pollution occurs; service station leaks and the discharge of minute amounts of pollutants in urban areas also add to the issue. The damage done by hydrocarbon pollution to the drinking water system in western Mexico City in April 2024 was an obvious example of this urban hazard (Barragán, 2024).

A tiny quantity of gasoline can contaminate vast amounts of water, whether because of natural spills or unintentional spills that occur during manufacture, transit, or storage. Gasoline-contaminated water needs to be treated since it is not suitable for residential use, human consumption, or irrigation. As is widely known, gasoline is a complex blend of hydrocarbons, among which benzene, toluene, and xylenes stand out, generally referred to as aromatics. According to the US Environmental Protection Agency (EPA), the maximum contaminant levels for these compounds are 5.0 ppb, 0.7 to 1.0 ppm, and 10 ppm, respectively (Meegoda and Hu, 2011). A 10 gallon spill of typical gasoline contains more than 200 g of benzene, which can contaminate millions of gallons of drinking water, exceeding recommended safe levels.

Depending on the size of the gasoline droplets, dispersions or emulsions may form, even though water and gasoline are normally chemically different and immiscible (Haan et al., 2023). A crucial factor influencing the stability and physicochemical behavior of gasoline–water emulsions is droplet size. While smaller droplets increase the interfacial area, improving mass transfer and dispersion stability, larger droplets encourage coalescence and phase separation, decreasing emulsion stability and changing transport properties.

Fortunately, there are many processes that can be implemented to remove gasoline from contaminated water. To be efficient, these processes must avoid the production of harmful secondary compounds. Thus, some conventional physicochemical methods, such as coagulation and flocculation, are out because they produce a large quantity of contaminated sludges. Other more innovative technologies are available, including thermal incineration, ultrasonic irradiation, microwave irradiation, nanofiltration, reverse osmosis, advanced catalytic oxidation, among others, which require large amounts of energy and currently have little industrial application (Mohammadi et al., 2020). Advanced oxidation processes (AOPs), which involve the production of unselective oxidizing agents especially hydroxyl radicals that aggressively attack organic molecules, represent another viable alternative, specifically in case necessitating the removal of BTEX (benzene, toluene, ethylbenzene, and xylenes) contaminants at low concentrations. However, its large-scale application requires the analysis of several factors, among which the following stand out: 1) high energy and reagents consumption; 2) need for specialized equipment, such as: UV sources, reactors, ozone generators, dosing systems of chemicals, power suppliers, etc.; 3) complexity of aqueous matrix, the presence of scavenging species several compromises the efficiency of the selected AOP; 4) high hydrocarbon concentration, generally an AOP is applied for tertiary treatment after bulk contaminant removal, since excessive amount of oxidants are needed; and 5) potential formation of by-products, when mineralization is not achieved leading to the formation of intermediate compounds, including oxidized aromatic compounds (Muvel et al., 2025).

In contrast, adsorption, which uses abundant natural minerals, high-quality synthetic materials, and low-cost natural adsorbents, is an emerging technology with real-world applications. This technology can be combined with more sophisticated methods, potentially reducing sludge production and lowering process costs. Adsorption alone can treat large volumes of effluent and achieve high removal rates using the appropriate adsorbent.

Adsorption can be carried out in a batch process using stirred tanks or in a continuous process using packed columns. In both cases, natural or synthetic materials are used as adsorbents. A batch process typically provides characterization of the adsorbent and kinetic, thermodynamic, and equilibrium data for the process, as well as the influence of various adsorption process parameters (pH, adsorbent dosage, stirring speed, temperature, etc.). Data such as maximum removal percentage, maximum removal capacity, and adsorption mechanism are easily obtained in batch processes. This information is valuable because it is used to design continuous processes. In a continuous process, it is possible to determine the mass transfer zone, column breakthrough time and saturation time, flow rate, and packed bed height. Furthermore, the process can be modeled for possible scale-up to a pilot plant and later to an industrial scale (Patel, 2021).

A wide variety of biosorbents have been used to remove crude oil and other hydrocarbons from water in a batch process, including eggshells, walnut shells, banana peels, coconut fiber, sawdust, palm fronds, and others (Muhammad et al., 2012; Buaban et al., 2024; Albatrni et al., 2022; El-Din et al., 2018; Cardoso et al., 2025; Meez et al., 2021; Zamparas et al., 2020). In the case of anise residue, a removal capacity of 30 $mg \cdot g^{-1}$ and a removal percentage of 70% are reported, while for the animal bone adsorbent, a capacity and a removal percentage of 45 mg·g^{-1} and 94% are reported, respectively (Al-Najar et al., 2023). On the other hand, there are natural adsorbents from the Earth's crust such as bentonite, sepiolite, attapulgite, chitosan, graphene oxide, among others, which have been used to remove oil from contaminated water with great success since, unlike the former, they are insoluble in water and have superior mechanical resistance properties (Haan et al., 2023). But without a doubt the adsorbent that has been used the most is activated carbon, for this material removal percentages higher than 97% are reported with removal capacities of 8.3 g·g^{-1} for gasoline emulsified in water (Asif et al., 2023). Nevertheless, its widespread application presents several limitations; preparing a material with high porosity requires physical or chemical treatment that make synthesis an energy-intensive process. The other major limitations with activated carbon in oil spill cleanups include lack of selective water molecules; other polar molecules can be attracted to its surface, causing limited surface sites of the adsorbent and limited regeneration for reusability. This implies the spent material must be subjected to a recovery process, which is often more expensive than the preparation because it may involve toxic substances (Satyam and Patra, 2024; Kosheleva et al. 2022).

Some results worth mentioning in a continuous process for removing hydrocarbons from water are, for example, the use of NaA zeolite nanoparticles with removal percentages of 87.4% (Esmaeili and Saremnia, 2018); the use of polymeric adsorbents with adsorption capacities of around 100 mg·g^{-1} (Al-Maas et al., 2022); the use of a mixture of activated carbon with silica gel with a removal percentage of 83.6% and an adsorption capacity of 108 mg·g^{-1} (Khader et al., 2021); or the use of pure activated carbon with a removal percentage of 96.7% (Kassob and Abbar, 2022).

Once it has been decided to evaluate the continuous process by manipulating the parameters of packed bed height, volumetric flow rate and initial concentration, through the experimental results of concentration versus time, it is possible to analyze the performance of the column through some simple models, such as the Thomas, Yoon-Nelson, Adams-Bohart, Wolborska, Dose-Response, Bed Depth Service Time models, among others.

The main objective of this study is to determine the operating and performance parameters for the removal of water-emulsified gasoline in a continuous process, using mexicalcite as the adsorbent material in a fixed-bed column.

Specifically, this work aims to:

1. Determine the breakthrough time at an effluent concentration of 10 mg·L^{-1} and the saturation time at an effluent concentration of 0.99C_0.
2. Quantify other crucial parameters, including the volume of emulsion treated at saturation, the mass transfer zone length, the overall removal percentage, and the adsorption capacity of the adsorbent.
3. Analyze the influence of key operating conditions—namely, the packed bed height, the volumetric flow rate, and the initial influent concentration on the adsorption process performance.
4. Model the breakthrough curves using established kinetic models: Thomas, Adams-Bohart, Wolborska, Dose-Response, and Yoon-Nelson equations.

2. MATERIAL AND METHODS

2.1. Preparation of the packed bed column with the adsorbent

Mexicalcite is a natural mineral obtained from mines located in the state of Oaxaca, Mexico. It is marketed by the company Lumogral S.A. de C.V. (Iztapalapa, Mexico City). The physicochemical characteristics of this mineral reported by the supplier are the following: apparent density of 1604 kg·m^{-3}; particle size distribution of 0.147 to 4.7 mm; 23.2% porosity;

4.5 µm pore diameter; 1132 $m^2 \cdot kg^{-1}$ of surface area; permeability of 2.7×10^3 $m \cdot s^{-1}$ and zero charge point at a pH value of 9.3. The compounds that have been identified in this material are calcite, quartz and calcium and magnesium silicate (Cruz-Olivares *et al.*, 2016). While the elemental composition is mainly composed of O (54.6%), C (12.4%), Ca (10.3%), Si (10.2%), Al (4.6%), Mg (3.2%), Fe (2.5%) and Na (0.5%) (Cruz-Olivares *et al.*, 2022). The adsorbent was previously sieved and the portion with a particle size distribution of 0.8 - 1.3 mm was used. A glass column 1.6 cm in diameter and 30 cm long was used. A cotton plug was placed to support the adsorbent inside the column.

2.2. Preparation of gasoline-water emulsions

For gasoline-water mixtures with concentrations of 500, 1000, and 1500 $mg \cdot L^{-1}$, 5, 10, and 15 g samples of regular 87-octane gasoline were weighed, and each was diluted with 1.0 L of distilled water (Turbidity = 2.3 NTU, electrical conductivity = 3.2 $\mu S \cdot cm^{-1}$, and pH = 6.5). In this study, water was used as the continuous phase and gasoline as the dispersed phase. Emulsions were prepared by gradually adding the required amount of gasoline to the aqueous phase, followed by homogenization using a Caframo mixer (BDC6016) operated at 2000 rpm for 30 s. The resulting emulsions contained dispersed phase weight fractions of 0.005, 0.010, and 0.015, respectively. The creaming test was used to assess the emulsions' stability (Ismaiel *et al.*, 2025). For the gasoline-in-water emulsions at concentrations of 500, 1000, and 1500 $mg \cdot L^{-1}$, the 24-hour creaming index findings were 3.6%, 4.0%, and 4.5%, respectively. These findings verify that the emulsions maintain their stability for the course of column adsorption tests, which last no more than four hours.

2.3. Determination of gasoline concentration in the effluent

The gasoline concentration was determined by a Total Organic Carbon analyzer (TOC-5050, Shimadzu) with a detection range of 5 to 10,000 $mg \cdot L^{-1}$. The samples were analyzed by duplicate.

2.4. Column adsorption process

The appropriate amount of adsorbent was placed inside the column to reach heights of 2 cm (4.45 g), 4 cm (9.92 g), and 6 cm (14.86 g). After that, adsorbent was washed with 300 mL of distilled water. Each emulsion was passed downward through the respective packed bed at flow rates of 5, 10, and 15 $mL \cdot min^{-1}$. The gasoline concentration at the column outlet was measured every 5 minutes until the saturation concentration was exceeded, which in this case was $0.99C_0$. The procedure for determining the adsorption capacity, removal percentage, and mass transfer zone in a packed column is well known. This procedure has been described in detail in several publications (Cruz-Olivares *et al.*, 2013; Marzbali and Esmaieli, 2017) and is briefly summarized here.

The maximum adsorption capacity of the column, q_{sat} (mg), requires the application of Equation 1, in which A represents the area under the C_{ads} curve as a function of time, t (min). The adsorbed concentration, C_{ads} ($mg \cdot L^{-1}$), is defined as difference between feed gasoline concentration, C_0 ($mg \cdot L^{-1}$), and column outlet gasoline concentration at any time, C_t ($mg \cdot L^{-1}$), by way of explanation, $C_{ads} = C_0 - C_t$. Other variables that appear in Equation 1 are: saturation time in the column, t_{sat} (min); and volumetric flow, Q ($mL \cdot min^{-1}$). It is relevant to note that the integral of Equation 1 can be solved numerically using any commercial software, such as Origin, and A is expressed in $mg \cdot min \cdot L^{-1}$.

$$q_{sat} = \frac{QA}{1000} = \frac{Q}{1000}\int_0^{t=t_{sat}} C_{ads}dt \qquad (1)$$

The adsorption capacity, q (mg·g^{-1}) is determined by Equation 2, dividing the maximum adsorption capacity, q_{sat}, by the mass of the adsorbent, w (g).

$$q = \frac{q_{sat}}{w} \tag{2}$$

The gasoline maximum mass retained in the column at the saturation time, m_{sat} is obtained with Equation 3.

$$m_{sat} = \frac{C_0 Q t_{sat}}{1000} \tag{3}$$

Then, the percentage of removal (%R) is obtained by means of Equation 4:

$$\%R = \frac{q}{m_{sat}} \times 100 \tag{4}$$

Finally, the mass transfer zone, MTZ (cm), was determined using Equation 5.

$$MTZ = Z\left(1 - \frac{t_b}{t_{sat}}\right) \tag{5}$$

Where t_b is the breakthrough time (min), namely the time required to reach 10 mg·L^{-1} gasoline concentration in the effluent.

2.5. Modeling of the adsorption process

To adequately model the dynamic behavior of the gasoline adsorption system in a column packed with mexicalcite, five kinetic models widely recognized in the scientific literature were used, these models are: Thomas, Adams-Bohart, Wolborska, Dose-Response, and Yoon-Nelson, which allow the evaluation of the maximum adsorption capacity, the adsorption kinetic constant, the minimum height of the packed bed, the time required for 50% of the emulsified gasoline to be adsorbed, the influence of mass transfer phenomena and the validation of the effects of the design variables, Z, Q and C_0. The equations and characteristics of these models are shown in the following paragraphs:

2.5.1. Thomas model

This model assumes that the adsorption kinetics is primarily of the Langmuir type, the circulation in the column is plug-like, the column is assumed to have no axial dispersion, and the second-order kinetics correspond to the driving force of adsorption (Equation 6).

$$Ln\left(\frac{C_0}{C_t} - 1\right) = \frac{K_{Th} q w}{Q} - K_{Th} C_0 t \tag{6}$$

Where C_0 and C_t are the inlet and outlet concentrations (mg·L^{-1}), K_{Th} is the Thomas constant (mL·mg^{-1}·min^{-1}), q is the adsorption capacity (mg·g^{-1}), w is the mass of adsorbent (g), Q is the volumetric flow (mL·min^{-1}) and t is time (min).

2.5.2. Adams – Bohart model

In this model it is supposed that there is no external resistance to particle propagation or mass transfer, the adsorption process is regulated by chemical interaction between the adsorbent surface and the adsorbate, both axial and radial dispersion are negligible, the proportion of free space in the packed bed is unchanged, the physical characteristics of the adsorbent and adsorbate remain unchanged and only applicable to dilute concentrations (Equation 7).

$$Ln\left(\frac{C_t}{C_0}\right) = K_{AB}C_0t - K_{AB}N_0\left(\frac{Z}{v}\right) \quad (7)$$

C_0 *and* C_t are the inlet and outlet concentrations ($mg \cdot L^{-1}$), $\mathbf{K_{AB}}$ is the Adams-Bohart constant ($L \cdot mg^{-1} \cdot min^{-1}$), N_0 is the saturation concentration (mg·L-1), Z is the packed bed height (cm), v is the linear flow rate (cm·min-1), and t is time (min.

2.5.3. Wolborska model

The behavior of this model is only valid in the initial stage of the breakthrough curve at low concentrations and axial propagation and external mass displacement contribute to the breakthrough curve (Equation 8).

$$Ln\left(\frac{C_t}{C_0}\right) = \left(\frac{\beta_a C_0}{N_0}\right)t - \frac{\beta_a Z}{v} \quad (8)$$

C_0 and C_t are the inlet and outlet concentrations ($mg \cdot L^{-1}$), β_α is the internal mass transfer kinetic constant (min^{-1}), N_0 is the saturation concentration ($mg \cdot L^{-1}$), Z is the packed bed height (cm), v is the linear flow rate ($cm \cdot min^{-1}$), and t is time (min).

2.5.4. Dose – Response model

This model is based on the fundamentals of mass transfer, it correctly explains the behavior of the breakthrough curve in very short and very long periods of operation, and it is more reliable to calculate the maximum adsorption capacity (Equation 9).

$$Ln\left(\frac{C_t}{C_0 - C_t}\right) = aLn(C_0Qt) - aLn(qw) \quad (9)$$

C_0 and C_t are the inlet and outlet concentrations ($mg \cdot L^{-1}$), a is a parameter of the Dose-Response model, q is the adsorption capacity ($mg \cdot g^{-1}$), w is the mass of adsorbent (g), Q is the volumetric flow ($mL \cdot min^{-1}$) and t is time (min).

2.5.5. Yoon – Nelson model

For this model the properties of the adsorbate and the adsorbent, together with the physical characteristics of the packed bed, do not affect the adsorption process, it is assumed that, both the probability of adsorption and the infiltration of the adsorbate into the adsorbent determine the rate of adsorption in a column of a given depth and the elements that determine the rate of adsorption in the column are adsorption and desorption (Equation 10).

$$Ln\left(\frac{C_t}{C_0 - C_t}\right) = K_{YN}t - K_{YN}\tau \quad (10)$$

C_0 and C_t are the inlet and outlet concentrations (mg·L-1), K_{YN} is the Yoon-Nelson constant ($L \cdot min^{-1}$), τ is time (min) required to decrease at 50% initial gasoline concentration and t is time (min).

2.6. Effect of the packed bed height, volumetric flow and the initial concentration

This study examined the impact of three factors on removal percentage and adsorption capacity: bed height (Z), flow rate (Q), and initial concentration (C_0) It only took seven experiments. An incomplete one-factor experimental design was employed for the independent assessment (without taking interactions into account) of the impact of these three factors on the process. In each subset of trials, this kind of design is distinguished by the fact that just one variable is changed while the others stay the same. Evaluation of factor (Z): Experiments 1, 2, and 3 varied bed height (2, 4, 6 cm) while flow rate ($5\ mL \cdot min^{-1}$) and concentration

(500 mg·L^{-1}) remained constant. Evaluation of factor (*Q*): Experiments 2, 4, and 5 varied volumetric flow (5, 10, 15 mL·min^{-1}) while packed bed height (4 cm) and concentration (500 mg·L^{-1}) remained constant. And evaluation of the factor (C_0): Experiments 2, 6, and 7 vary (500, 1000, 1500 mg·L^{-1}) while (4 cm) and (5 mL·min^{-1}) remain constant.

3. RESULTS AND DISCUSSION

3.1. Performance of the adsorbent

From the results shown in Table 1, mexicalcite is an adsorbent with outstanding characteristics for removing gasoline from water. This material shows an average adsorption capacity of 60.25 mg·g^{-1}. With a mass transfer zone of only 0.95 cm, it can process 921 mL of effluent, with a breakthrough time (period in which the gasoline concentration at the column outlet is equal or less than 10 mg·L^{-1}) of 114 min, and a saturation time of 146 min. On average, it can remove 90.5% of the gasoline contained in aqueous mixtures with concentrations between 500 and 1500 mg·L^{-1}.

Table 1. Experimental results of gasoline removal with mexicalcite.

Experiment number	%*R*	Q (mg·g^{-1})	t_b (min)	t_{sat} (min)	V_{eff} (mL)	*MTZ* (cm)
1	85.3±3.6	36.19±2.05	60±2.5	94±4.0	470±6.6	0.72±0.03
2	94.6±4.0	37.44±2.12	130±5.5	164±7.0	820±11.6	0.83±0.04
3	95.0±4.0	38.68±2.19	196±25.5	229±6.5	1145±16.2	0.86±0.04
4	86.4±3.7	43.60±1.85	65±2.8	99±4.2	990±14.0	1.37±0.06
5	80.0±3.4	54.51±3.08	51±2.2	85±3.6	1275±18.0	1.6±0.07
6	95.0±4.0	79.07±3.35	135±25.7	166±7.0	830±11.7	0.75±0.03
7	97.1±4.1	132.23±5.61	159±6.7	183±5.2	915±12.9	0.52±0.02
Average	90.5±3.8	60.25±2.89	114±4.4	146±5.3	921±13.0	0.95±0.04

* The standard deviation of average values is presented.

Regarding the removal of crude oil, oils, and other hydrocarbons from aqueous mixtures, mexicalcite shows results like those of most bioadsorbents, synthetic adsorbents, and inorganic adsorbents. For example, using banana rachis with a particle size of 850 µm, adsorption capacities of 6.26 g·g^{-1} and 6.61 g·g^{-1} are reported for gasoline and diesel, respectively (Vera-Infante et al., 2023), also anise residue has been reported to remove 70% of hydrocarbons with an adsorption capacity of 30 mg·g^{-1} (Al-Najar et al., 2023). Other natural inorganic adsorbents, such as bentonite and montmorillonite, show hydrocarbon removal capacities of 7.12 mg·g^{-1} and 5.8 mg·g^{-1}, respectively (Okiel et al., 2011; Akpomie et al., 2019). Recent advancements in material science have enabled clay modification, leading to enhanced adsorption performance, Fe_2O_3/bentonite composite demonstrated a high removal capacity of 249.46 mg·g^{-1} for gasoline in water (Sarran et al., 2024); other result reports that the incorporation of montmorillonite into xanthan esterified with acrylic acid polymer matrix, can remove degraded motor oil with a capacity of 45.73 g·g^{-1} (Apostol et al., 2024); nevertheless, the pretreatment of the raw clay contributes to higher costs. Removal percentages of 93% and 87%, respectively, are also reported for synthetic inorganic adsorbents such as silica nanoparticles and carbon nanotubes doped with iron oxide (Franco et al., 2014; Fard et al., 2016).

3.2. Effect of Z (Experiments 1, 2, and 3)

Increasing the packed bed height had a positive effect on the removal percentage and adsorption capacity, evidenced by data in Table 1 (experiments 1, 2, and 3). These three experiments were carried out at three different packed bed heights: 2, 4, and 6 cm, corresponding to 4.45, 9.92, and 14.86 g of adsorbent, respectively, at a flow rate of 5 mL·min^{-1} and an inlet concentration of 500 mg·L^{-1}. Analyzing the results of removal percentage and adsorption capacity, it is apparent that by doubling the value of the packed bed height, the percentage and adsorption capacity increase by 10.9% and 3.5%, respectively, while by tripling the packed bed height, the $\%R$ and q increase by 11.4% and 6.9%, respectively. This is because increasing the height of the packed bed increases the contact time between the phases, allowing gasoline molecules more time to diffuse through the pores of the mexicalcite, thereby increasing the mass transfer zone and the volume of treated effluent. This behavior is widespread in column adsorption processes (Marzbali and Esmaieli, 2017). As illustrated in Figure 1, both the breakthrough time and saturation time increase with increasing packed bed height.

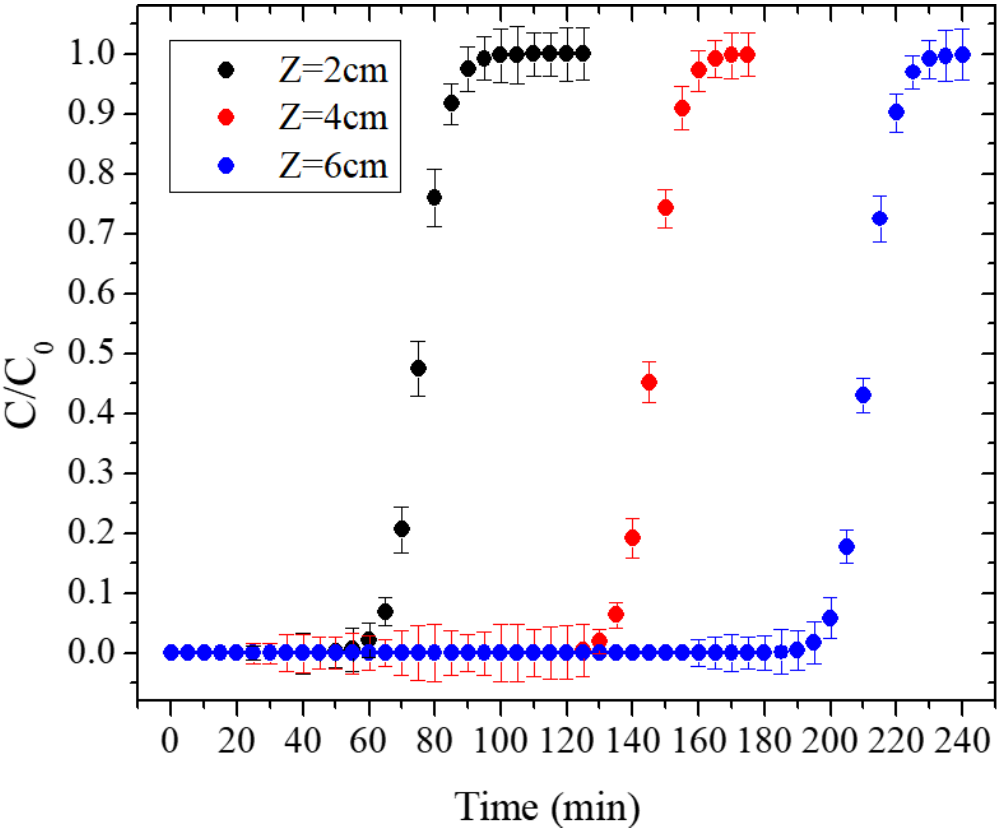

Figure 1. Breakthrough curves for gasoline adsorption (C/C0 vs time) at different packed bed heights, including experimental error bars.

3.3. Effect of *Q* (Experiments 2, 4 and 5)

The data presented in Table 1 indicate that increasing the volumetric flow rate positively affects adsorption capacity and negatively affects removal percentage (experiments 2, 4, and 5). These three experiments were carried out at three different volumetric flow rates: 5, 10, and 15 mL·min^{-1}. The packed bed height was maintained at 4 cm (9.92 g of adsorbent) and the inlet concentration was 500 mg·L^{-1}. Analyzing the results of removal percentage and adsorption capacity, by doubling the volumetric flow the adsorption capacity increases by 16.5% and the removal percentage decreases by 8.7%, while by tripling the volumetric flow the adsorption capacity increases by 45.6% and the removal percentage decreases by 15.4%. This is because increasing the volumetric flow rate decreases the contact time between the phases, as well as the breakthrough time and saturation time. This behavior has also been reported in the arsenic adsorption process (Yunnen et al., 2017).

Figure 2 reveals both the breakthrough time and saturation time decrease dramatically with increasing volumetric flow rate.

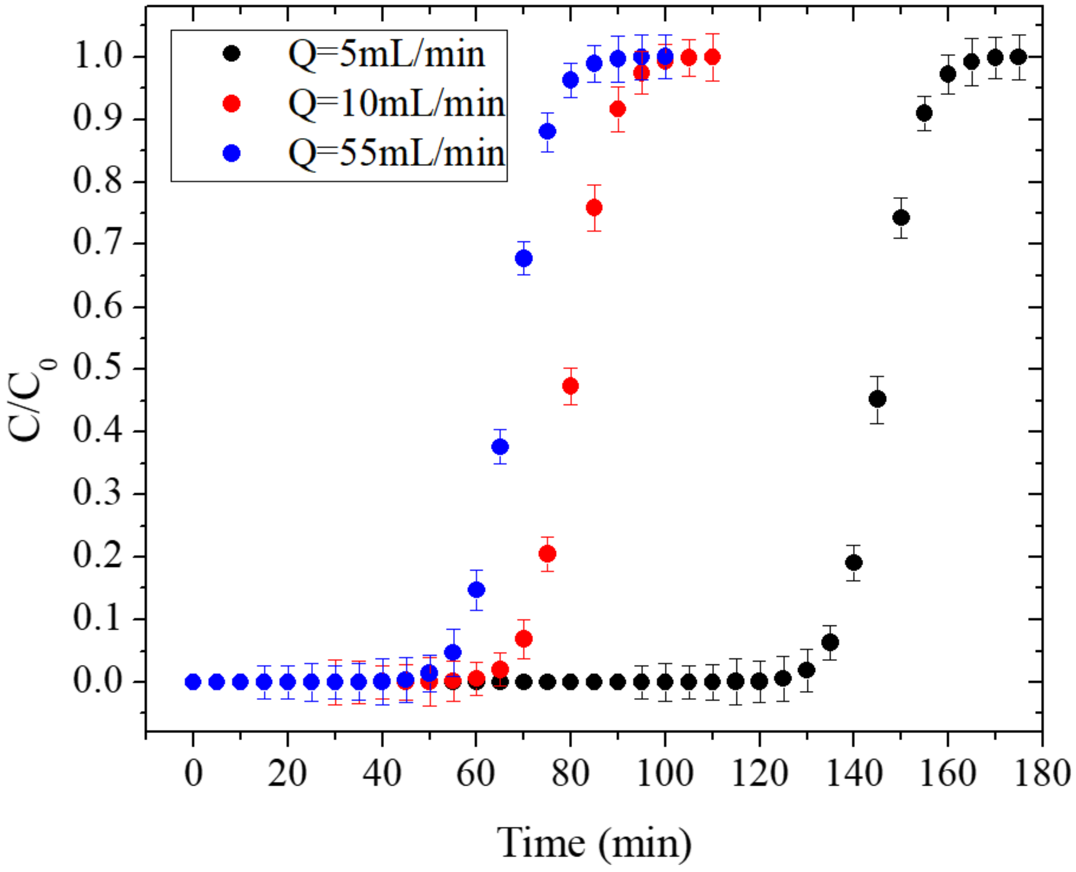

Figure 2. Breakthrough curves for gasoline adsorption (C/C0 vs time) at different flow rates, including experimental error bars.

3.4. Effect of C_0 (Experiments 2, 6 and 7)

Increasing the initial concentration had a positive effect on the removal percentage and adsorption capacity, as detailed in Table 1 (experiments 2, 6, and 7). These three experiments were carried out at three different initial concentrations: 500, 1000, and 1500 mg·L^{-1}. The packed bed height was maintained at 4 cm (9.92 g of adsorbent) and the volumetric flow rate was 5 mL·min^{-1}. The removal percentage and adsorption capacity results indicate that by doubling the initial concentration value, the removal percentage and adsorption capacity increase by 0.42% and 111%, respectively, while by tripling the height of the packed bed, the *%R* and *q* increase by 2.6% and 253%, respectively. This is because as the initial concentration increases, the gasoline concentration gradient between the liquid and the adsorbent surface increases, and therefore, there is a greater mass transfer of gasoline between the phases, which is reflected in an increase in the service time of the column.

As can be seen in Figure 3, both the breakthrough time and the saturation time increase with increasing initial concentration.

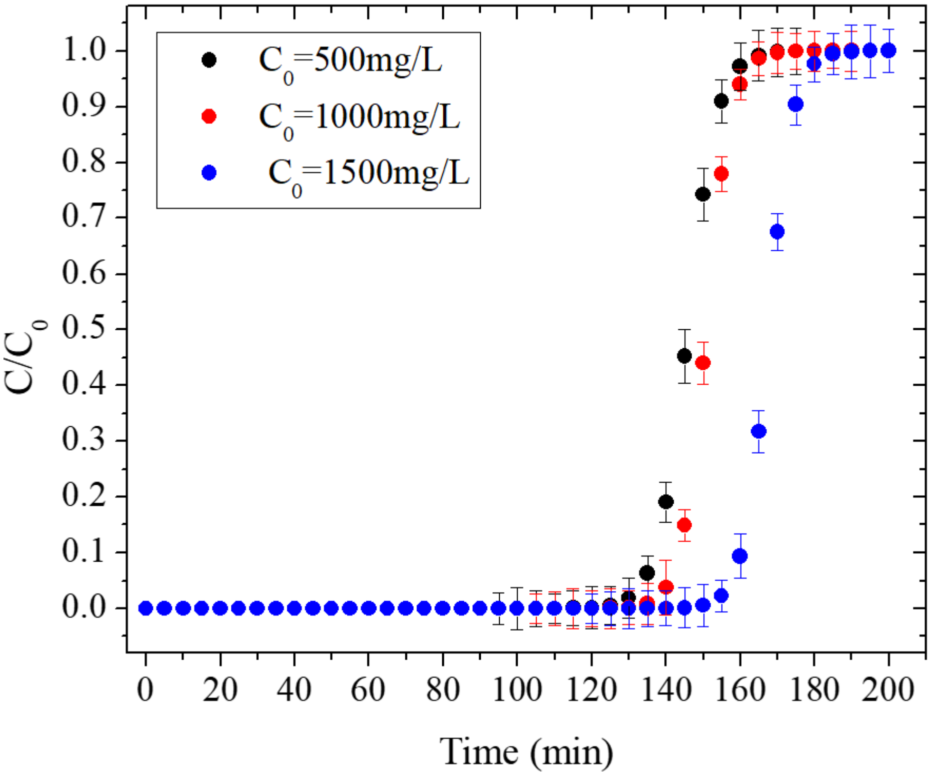

Figure 3. Breakthrough curves for gasoline adsorption (C/C0 vs time) at different initial concentrations, including experimental error bars.

3.5. Modeling process

The dynamic behavior of the column was satisfactorily adjusted to the Thomas, Adams-Bohart, Wolborska, Dose-Response and Yoon-Nelson models; in all cases, the quadratic correlation factor is greater than 0.99, as demonstrated by Table 2.

Table 2. Column adsorption process parameters according to the models used for gasoline removal.

Model	Experiment number	*q* (mg·g^{-1})	K_{Th}×10^4 (mL·mg^{-1}·min^{-1})	R^2	*AARD*(%)
Thomas	1	35.186	4.992	0.999	1.47
	2	36.436	4.984	0.998	2.44
	3	37.672	5.026	0.997	3.22
	4	40.197	4.984	0.999	4.55
	5	50.265	5.006	0.998	1.27
	6	75.413	3	0.996	1.61
	7	125.677	1.999	0.999	1.04
Model	**Experiment number**	N_0 (mg·L^{-1})	K_{AB}×10^4 (mL·mg^{-1}·min^{-1})	R^2	*AARD(%)*
Adams – Bohart	1	28106.96	4.804	0.998	2.80
	2	29254.409	4.812	0.998	7.20
	3	30523.952	4.922	0.998	5.52
	4	32528.582	4.802	0.999	4.22
	5	40504.026	4.9	0.999	5.04
	6	60349.509	2.925	0.998	5.90
	7	100367.425	1.965	0.999	4.25

Continue...

Continued...

Model	Experiment number	N_0 (mg·L^{-1})	β_a (min^{-1})	R^2	*AARD*(%)
Wolborska	1	28106.96	13.834	0.998	2.80
	2	29254.409	14.077	0.998	7.20
	3	30523.952	14.664	0.998	5.52
	4	32528.582	15.62	0.999	4.22
	5	40504.026	19.847	0.999	5.04
	6	60349.509	17.652	0.998	5.90
	7	100367.425	19.719	0.999	4.22
Model	Experiment number	q (mg·g^{-1})	a	R^2	*AARD(%)*
Dose – Response	1	34.446	14.14	0.99	17.31
	2	34.996	29.173	0.994	5.55
	3	37.249	49.684	0.997	10.35
	4	36.974	15.075	0.986	13.92
	5	46.654	11.621	0.992	13.73
	6	75.051	40.595	0.996	15.75
	7	125.31	45.126	0.996	10.62
Model	Experiment number	τ (min)	K_{YN} (min^{-1})	R^2	*AARD(%)*
Yoon – Nelson	1	75.344	0.2496	0.999	1.75
	2	145.746	0.2492	0.999	2.73
	3	211.118	0.2513	0.999	4.00
	4	80.393	0.2492	0.998	1.96
	5	67.019	0.2503	0.999	1.52
	6	150.827	0.3	0.997	1.69
	7	167.569	0.2999	0.999	1.12

These models provide valuable information about the adsorption process. For example, the Thomas and Dose-Response models provide the adsorption capacity of the adsorbent (q). In this case, for mexicalcite, the adsorption capacity obtained with the Thomas model has an average difference of 4.7%, expressed as a percentage of relative error. With the Dose-Response model, the difference is 7.9% compared to the experimental results. On the other hand, with the Adams-Bohart and Wolborska models saturation concentration (N_0) or final concentration of the effluent is obtained, with both models the adjustment of the experimental data has a quadratic correlation (R^2) greater than 0.99. With the Yoon-Nelson model the time in which the concentration of the solute at the column outlet has fallen to half the value of the initial concentration (τ) is obtained, in this case, the percentage of relative error of the comparison of τ obtained by the Yoon-Nelson model and that obtained experimentally is less than 3% on average. The percentage of the average absolute relative deviation (*AARD*) is shown in Table 2. This percentage was obtained from the comparison between experimental concentration and the one calculated using the kinetic models.

A comparison between the experimental adsorption capacities and those predicted by the Thomas and Dose-Response models is presented in Table 3. The corresponding mean percentage deviations were 4.75% for the Thomas model and 7.86% for the Dose-Response model.

Table 3. Comparison between experimental adsorption capacity values and those derived from models.

Experiment number	*q* exp (mg·g^{-1})	*q* Thomas (mg·g^{-1})	Deviation (%)	*q* Dose-Response (mg·g^{-1})	Deviation (%)
1	36.19±2.05	35.19	2.77	34.45	4.82
2	37.44±2.12	36.44	2.68	35.00	6.53
3	38.68±2.19	37.67	2.61	37.25	3.70
4	43.60±1.85	40.20	7.81	36.97	15.20
5	54.51±3.08	50.27	7.79	46.65	14.41
6	79.07±3.35	75.41	4.63	75.05	5.08
7	132.23±5.61	125.68	4.96	125.31	5.23
Average	60.25±2.89	57.26	4.75	55.81	7.85

4. CONCLUSIONS

Mexicalcite is a low-cost, low-conditioning natural mineral capable of efficiently removing gasoline mixed with water in a continuous packed-bed column process. On average, mexicalcite adsorbs 60.25 mg of gasoline per gram of adsorbent, achieving a removal rate of 90.5%. The highest removal rate (97.1%) and maximum adsorption capacity (132.23 mg·g^{-1}) were obtained with a packed-bed height of 4 cm, a volumetric flow rate of 5 mL·min^{-1}, and an initial concentration of 1500 mg·L^{-1}. Under these experimental conditions, the breakthrough time was 159 min, the saturation time was 183 min, the treated effluent volume was 915 mL, and the mass transfer zone was 0.52 cm. The most important effect on the removal percentage and adsorption capacity is the volumetric flow rate, since it directly influences the breakthrough time and the saturation time of the column.

All the models tested in this study to describe the dynamic behavior of the column do so satisfactorily because in all cases the quadratic correlation (R^2) was greater than 0.99.

5. DATA AVAILABILITY STATEMENT

Data availability not informed.

6. REFERENCES

AKPOMIE, K. G.; ONYEABOR, C. F.; EZEOFOR, C. C.; ANI, J. U.; EZE, S. I. Natural aluminosilicate clay obtained from south-eastern Nigeria as potential sorbent for oil spill remediation. **Journal of African Earth Sciences**, v. 155, p. 118-123, 2019. https://doi.org/10.1016/j.jafrearsci.2019.04.013

ALBATRNI, H.; QIBLAWEY, H.; AL-MARRI, M. J. Walnut shell based adsorbents: A review study on preparation, mechanism, and application. **Journal of Water Process Engineering**, v. 45, 2022. https://doi.org/10.1016/j.jwpe.2021.102527

AL-MAAS, M.; MINIER-MATAR, J.; KRUPA, I.; AL-MAADEED, M. A. A.; ADHAM, S. Evaluation of polymeric adsorbents via fixed-bed columns for emulsified oil removal from industrial wastewater. **Journal of Water Process Engineering,** v. 49, n. 102962, p. 1-13, 2022. https://doi.org/10.1016/j.jwpe.2022.102962

AL-NAJAR, J. A.; AL-HUMAIRI, S.T.; LUTFEE, T.; BALAKRISHNAN, D.; VEZA, I.; SOUDAGAR, M. E. M. *et al.* Cost-Effective Natural Adsorbents for Remediation of Oil-Contaminated Water. **Water**, v. 15, n 1186. p. 1-23, 2023. https://doi.org/10.3390/w15061186

APOSTOL, I.; DINU, M. V.; ANGHEL, N.; SPIRIDON, I. A green approach to oil spill mitigation: New hybrid materials for wastewater treatment. **Polymers**, v. 16, 2024. https://doi.org/10.3390/polym16152225

ARELLANO, A. México: consecuencias ambientales del derrame de petróleo que Pemex minimizó. **Mongabay**, 11 Aug. 2023. Available at: https://es.mongabay.com/2023/08/mexico-consecuencias-ambientales-del-derrame-de-petroleo-que-pemex-minimizo/. Access: 2025, Nov. 09.

ASIF, M.; BOUMAZA, M. M.; KUMAR, N. S.; AL-GHURABI, E. H.; SHAHABUDDIN, M. Adsorptive Removal of Emulsified Automobile Fuel from Aqueous Solution. **Separations**, v. 10, n. 493. p. 1-25, 2023. https://doi.org/10.3390/separations10090493

BARRAGÁN, A. Científicos de la UAM encuentran “compuestos orgánicos derivados del petróleo” en el agua contaminada de Benito Juárez. **El país**, México, 17-04-2024. https://elpais.com/mexico/2024-04-18/cientificos-de-la-uam-encuentran-compuestos-organicos-derivados-del-petroleo-en-el-agua-contaminada-de-benito-juarez.html. Access: 2025, Nov. 09.

BUABAN, R.; PATTANPORNPONG, K.; DOKSOY, T.; LORYUENYONG, V. Optimization of oil adsorption by using eggshell as an oil adsorbent. **Advances in Science and Technology**, v. 150, p. 39-44, 2024. https://doi.org/10.4028/p-23OkFm

CARDOSO, C. K. M.; MOREIRA, Í. T. A.; QUEIROZ, A. F. S.; OLIVEIRA, O. M. C. de; LOBATO, A. K. de C. L. Multiscale evaluation of raw coconut fiber as biosorbent for marine oil spill remediation: from laboratory to field applications. **Resources**, v. 14, n. 159, 2025. https://doi.org/10.3390/ resources14100159

CRUZ-OLIVARES, J.; MARTÍNEZ-BARRERA, G.; PÉREZ-ALONSO, C.; BARRERA-DÍAZ, C. E.; CHAPARRO-MERCADO, M. C.; UREÑA-NÚÑEZ, F. Adsorption of Lead Ions from Aqueous Solutions Using Gamma Irradiated Minerals. **Journal of Chemistry**, p. 1-7, 2016. https://doi.org/10.1155/2016/8782469

CRUZ-OLIVARES, J.; PÉREZ-ALONSO, C.; MARTÍNEZ-BARRERA, G.; ROA-MORALES, G.; LÓPEZ-TÉLLEZ, G.; MARTÍN DEL CAMPO-LÓPEZ, E. Modeling and scaling up of the Cr (VI) adsorption process by using mexicalcite natural mineral in a packed bed column. **Results in Engineering**, v. 16, n 100687, p. 1-9, 2022. https://doi.org/10.1016/j.rineng.2022.100687

CRUZ-OLIVARES, J.; PÉREZ-ALONSO, C.; BARRERA-DÍAZ, C.; UREÑA-NUÑEZ, F., M. C.; CHAPARRO-MERCADO, M. C.; BILYEU, B. Modeling of lead (II) biosorption by residue of allspice in a fixed-bed column. **Chemical Engineering Journal**, v. 228, p. 21–27, 2013. https://doi.org/10.1016/j.cej.2013.04.101

EL-DIN, G. A.; AMER, A. A.; MALSH, G.; HUSSEIN, M. Study on the use of banana peels for oil spill removal. **Alexandria Engineering Journal**, v. 57, n. 3, p. 2061-2068, 2018. https://doi.org/10.1016/j.aej.2017.05.020

ESMAEILI, A.; SAREMNIA, B. Comparison study of adsorption and nanofiltration methods for removal of total petroleum hydrocarbons from oil-field wastewater. **Journal of Petroleum Science and Engineering**, v. 171, p. 403-413, 2018. https://doi.org/10.1016/j.petrol.2018.07.058

FARD, A. K.; RHADFI, T.; MCKAY, G.; AL-MARRI, M.; ABDALA, A.; HILAL, N. Enhancing oil removal from water using ferric oxide nanoparticles doped carbon nanotubes adsorbents. **Chemical Engineering Journal**, v. 293, p. 90-101, 2016. http://dx.doi.org/10.1016/j.cej.2016.02.040

FRANCO, C. A.; NASSAR, N. N.; CORTÉS, F. B. Removal of oil from oil-in-saltwater emulsions by adsorption onto nano-alumina functionalized with petroleum vacuum residue. **Journal of Colloid and Interface Science**, v. 433, p. 58-67, 2014. http://dx.doi.org/10.1016/j.jcis.2014.07.011

HAAN, T. Y.; NORDIN, P. M. I.; JUANDA, N. I. A.; SHAFI, M. A. M.; KRISHNAN, P. A Review on Adsorption Process for the Treatment of Oily Wastewater. **Advances in Environmental and Engineering Research**, v. 4, n 1. p. 1-21, 2023. http://dx.doi.org/10.21926/aeer.2301016

ISMAIEL, L.; RIZZO, V.; DI MATTIA, C.; FANESI, B.; LUCCI, P.; D'ALESSIO, G. *et al.* Oil-in-water emulsions made of pistachio oil: physical and chemical properties and stability. **Foods**, v. 14, n. 60, 2025. https://doi.org/10.3390/foods14010060

KHADER, E. H.; MOHAMMED, T. J.; ADNAN, S. W. Reduction of oil and COD from produced water by activated carbon, zeolite, and mixed adsorbents in a fixed-bed column. **Desalination and Water Treatment,** v. 227, p. 216–227, 2021. https://doi.org/10.5004/dwt.2021.27295

KASSOB, A. N.; ABBAR, A. H. Treatment of petroleum refinery wastewater by adsorption using activated carbon fixed bed column with batch recirculation mode. **Al-Qadisiyah Journal for Engineering Sciences,** v. 15 p. 102–112, 2022. https://doi.org/10.30772/qjes.v15i2.820

KOSHELEVA, R. I.; KYZAS, G. Z.; KOKKINOS, N. C.; MITROPOULOS, A. C. Low-cost activated carbon for petroleum products clean-up. **Processes**, v. 10, n. 2, 2022. https://doi.org/10.3390/pr10020314

MARZBALI, M. H.; ESMAIELI, M. Fixed bed adsorption of tetracycline on a mesoporous activated carbon. Experimental study and neuro-fuzzy modeling. **Journal of Applied Research and Technology**, v. 15, p. 454 – 463, 2017. https://doi.org/10.1016/j.jart.2017.05.003

MEEGODA, J. N.; HU, L. A review of centrifugal testing of gasoline contamination and remediation. **International Journal of Environmental Research Public Health**, v. 8, n. 8, p. 3496-3513, 2011. https://doi.org/10.3390/ijerph8083496

MEEZ, E.; HOSSEINI-BANDEGHARAEI, A.; RAHDAR, A.; THYSIADOU, A.; MATIS, K. A.; KYZAS, G. Z. Synthetic Oil-Spills Decontamination by Using Sawdust and Activated Carbon from Aloe vera as Absorbents. **Biointerface Research in Applied Chemistry**, v. 11, n. 4, p. 11778-11796, 2021. https://doi.org/10.33263/BRIAC114.1177811796

MUHAMMAD, I. M.; EL-NAFATY, U. A.; ABDULSALAM, S.; MAKARFI, Y. I. Removal of oil from oil produced water using eggshell. **Civil and Environmental Research**, v. 2, n. 8, p. 52-63, 2012.

MOHAMMADI, L.; RAHDAR, A.; BAZRAFSHAN, E.; DAHMARDEH, H.; HASAN SUSAN, M. A. B. *et al.* Petroleum Hydrocarbon Removal from Wastewaters: A Review. **Processes**, v. 8, n. 447, p. 1-36, 2020. https://doi.org/10.3390/pr8040447

MORALES, F. Derrame de hidrocarburo contamina ocho kilómetros del río Pantepec en Veracruz. **Proceso**, 21 Oct. 2025. Available at: https://www.proceso.com.mx/nacional/estados/2025/10/21/derrame-de-hidrocarburo-contamina-ocho-kilometros-del-rio-pantepec-en-veracruz-video-361250.html Access: 2025, Nov. 09.

MUVEL, H.; JINDAL, M. K.; TEWARI, P. K.; ANAND, V. Minimizing oil pollution: a review of current status and its treatment options. **RSC Sustainability**, v. 3, p. 3681-3723, 2025. https://doi.org/10.1039/D5SU00403A

OKIEL, K.; EL-SAYED, M.; EL-KADY, M. Y. Treatment of oil water emulsions by adsorption onto activated carbon, bentonite and deposited carbon. **Egyptian Journal of Petroleum**, v. 20, p. 9-15, 2011. https://doi.org/10.1016/j.ejpe.2011.06.002

PATEL, H. Comparison of batch and fixed bed column adsorption: a critical review. **International Journal of Environmental Science and Technology**, v. 19, p. 10409–10426, 2021. https://doi.org/10.1007/s13762-021-03492-y

SARRAN, M. A.; ABDULRAZAK, A. A.; ABID, M. F.; JAWAD AL-BAYATI, A. D.; RASHID, K. T.; SHEHAB, M. A. *et al.* Oily wastewater treatment by using Fe_3O_4/bentonite in fixed-bed adsorption column. **ChemEngineering**, v. 8, n. 92, 2024. https://doi.org/10.3390/chemengineering8050092

SATYAM, S.; SANJUKTA, P. Innovations and challenges in adsorption-based wastewater remediation: A comprehensive review. **Heliyon**, v. 10, n. 9, 2024. https://doi.org/10.1016/j.heliyon.2024.e29573

VERA-INFANTE, T.; FERRER-GUTIÉRREZ, J. P.; GADVAY-YAMBAY, K. A.; BLACIO-TORO, S. E.; CUENCA-MAYORGA, F. P. Materiales absorbentes elaborados a partir de residuos de la agroindustria del banano, arroz y cacao destinados a la captación de hidrocarburos. **Acta Agronómica**, v. 72, n 2, p. 117-124, 2023. https://doi.org/10.15446/acag.v72n2.111928

YUNNEN, C.; YE, W.; CHEN, L.; LIN, G.; JINXIA, N.; RUSHAN, R. Continuous fixed-bed column study and adsorption modeling: Removal of arsenate and arsenite in aqueous solution by organic modified spent grains. **Polish Journal of Environmental Studies**, v. 26, n 4, p. 1847-1854, 2017. https://doi.org/10.15244/pjoes/68869

ZAMPARAS, M.; TZIVRAS, D.; DRACOPOULOS, V.; IOANNIDES, T. Application of Sorbents for Oil Spill Cleanup Focusing on Natural-Based Modified Materials: A Review. **Molecules**, v. 25, n. 19, 2020. https://doi.org/10.3390/molecules25194522